DOE/ER/45250--3

DE90 012248

INVESTIGATION ON THE MBE GROWTH AND PROPERTIES OF AlGaInAs/InP and InGaAs-InAlAs SUPERLATTICES

Final Report

for Period April 15, 1986 - December 14, 1989

P. K. Bhattacharya
R. Gibala

The University of Michigan
Departments of Electrical Engineering and Computer Science
and Materials Science and Engineering
Ann Arbor, Michigan 48109-2122

December 1989

Prepared for

THE U.S. DEPARTMENT OF ENERGY
AGREEMENT NO. DE-FG02-86ER45250

SUMMARY

The results presented in this report cover work carried out under grant DE-FG02-86ER45250 during the period May 15, 1986 to December 14, 1989. The focus of the work has been to grow wide-bandgap ternary and quaternary semiconductors InAlAs and InGaAlAs by molecular beam epitaxy and to investigate their electronic, optical and structural characteristics. The techniques being used are X-ray, TEM, photoluminescence and absorption, DLTS, Hall transport, and Raman Spectroscopy. The experiments have included both latttice matched and strained layers. We have grown a series of InGaAlAs quaternary alloys lattice matched to InP, covering the bandgap range from 0.75 to 1.45 eV. Low temperature photoluminescence measurements indicate that the layers are possibly the best even grown. The excitonic linewidths are extremely narrow and indicate minimal amounts of clustering. The extent of this clustering has been estimated from analysis of Hall data. The hole lifetimes in the alloys are comparable to those in high-purity GaAs. Deep levels in these alloys have been investigated and several dominant trap centers have been identified. Traps similar to the D-X center in AlGaAs are identified once the L-X mimina in strain InAlAs come below the Γ minimum in energy. This result is extremely significant and establishes conclusively the fact that the class of defects termed the D-X centers derive their unique properties from the bandstructure. Interdiffusion phenomena at InGaAs/InAlAs heterointerfaces have been studied and interpreted for the first time.

Detailed structural characterization of strained InGaAs/InAlAs on GaAs, by TEM has been done. The purpose of this study was two-fold: first, to understand the growth kinetics during strained epitaxy and the generation and propagation of dislocations; and second, to study the growth of thick mismatched layers for device applications. We have conclusively established that for large misfits ($\geq 1.5\%$) and (100) growth, 3-D island growth mode is energetically favored. The general nature of the misfit dislocation network at the InGaAs/GaAs interface is an orthogonal array. We have been, with the help of plan-view TEM measurements, able to relate the interfacial misfit dislocations with the surface cross-hatched pattern usually seen on strained layers. It is also seen that the dislocations propogate and multiply by a mechanism proposed by Hagen and Strunk. Finally, we have used mismatched and pseudomorphic and mismatched InGaAs on GaAs to realize state-of-art MODFETs and a novel bipolar transistor.

I. INTRODUCTION

The investigations and results being reported here stem directly from our efforts in understanding the molecular beam epitaxial growth, and the electrical, optical, and structural properties of In-bearing ternary and quaternary alloys grown on InP and GaAs substrates. The materials that have been investigated therefore include both lattice-matched and strained compounds. In the case of the former, the objective has been to understand and perfect the growth conditions and elucidate the parameters required for ideal compounds and heterostructures. In the case of the strained layers, emphasis has been laid on understanding the growth modes during strained layer epitaxy, their relation to the optical properties of heterostructures and the generation and propogation of dislocations in mismatched epitaxial layers. The work can therefore be divided into the following broad areas. First, we have investigated the growth of lattice-matched $In_{0.53}Ga_{0.47}As$, $In_{0.52}Al_{0.48}As$, and InGaAlAs on InP, clustering in these compounds, their optical properties and the behavior of dominant traps in these materials with respect to the changing bandstructure. We have studied in detail interdiffusion phenomena at the InGaAs/InAlAs interface for the first time and have found a "Darken"-like effect to be operative.

The other focal point of our investigations has been the understanding of the MBE growth and structural properties of strained InGaAs (or InAlAs) on GaAs and InP. We have, for the first time, shown that for large enough misfits, strained layers thermodynamically prefer to grow in a 3-D island mode. We have related the growth modes and growth parameters to critical thickness and dislocation formation. More importantly, we have studied the generation and propagation of misfit dislocations and have tried to relate them to surface morphology. These studies were made possible by high-resolution TEM measurements. We have applied the TEM techniques to other mismatched heterostructures such as GaAs/Al/GaAs and GaAs on sapphire. Finally, we have applied mismatched and pseudomorphic InGaAs layers and appropriate heterostructures to the realization of field effect transistors (FETs) and a novel bipolar transistor. In the case of the modulation doped FET we show that the material and device characteristics obtained with a highly mismatched channel is almost identical to state-of-art lattice-matched devices. This has been possible because of a good understanding of dislocation propogation and their suitable control. The important results are described in more detail in the following sections.

II. PROPERTIES OF LATTICE MATCHED $In_{0.53}(Ga_xAl_{1-x})_{0.47}As$/InP ALLOYS ON InP

2.1 Molecular Beam Epitaxial Growth

The $In_{1-x-y}Ga_xAl_yAs$ quaternary and ternary (x=0, y=0.48) alloys are impor-

tant materials for heterostructure optoelectronic and microwave devices. Previous work indicates that the molecular beam epitaxially (MBE) grown crystals may have significant clustering due to a predicted miscibility gap in the phase diagram for growth below 800°C. We have made a systematic study of the electrical and optical properties of these alloys grown by molecular beam epitaxy under different growth conditions. The specific experiments performed were low-temperature photoluminescence, minority carrier lifetime, and deep level transient spectroscopy (DLTS).

The most important considerations for the growth of high-quality crystals are: (i) source purity, (ii) growth parameters, and (iii) lattice-matching to the substrate. We have prebaked the highest purity commercially available In in a hydrogen ambient at 700°C for 24 hour before loading it into the growth chamber. It was then baked, together with the other source materials, in ultrahigh vacuum. The InAlAs alloys were grown at an elevated temperature of 520°C and a growth rate of ~ 1.2 μm/h, to reduce clustering effects. The growth parameters for the quaternary alloys were varied with composition. To ensure near-perfect lattice matching ($\Delta a/a_o < 10^{-4}$), the reflection high-energy electron diffraction (RHEED) intensity was monitored during growth. Si doping was used to achieve n-type materials. The electrical characteristics of the quaternary samples are shown in Table I.

Low-temperature photoluminescence (PL) measurements were made on the ternary and quaternary samples. The main peak in the PL spectra is probably composed of donor and acceptor related bound excitons. The best linewidth (FWHM) that we have obtained for the ternary alloy is 12.8 meV at 15 K. In the quaternary with composition $In_{0.53}Ga_{0.30}Al_{0.17}As$, a linewidth of 6.6 meV is measured. These numbers are among the lowest achieved to date. Photoluminescence data of the ternary and quaternary alloys are shown in Figs. 1 and 2, respectively. We believe that in the ternary alloys, linewidths close to the theortical (no clustering) limit of 4.1 meV can be achieved.

Table I. Electrical properties of InGaAlAs grown by MBE.

				Electron traps		
Sample	Band gap (RT)(eV)	n (cm^{-3})	μ(300K) (cm^2/Vs)	N_T (cm^{-3})	σ_∞ (cm^2)	ΔE_T (eV)
$In_{0.53}Ga_{0.42}Al_{0.05}As$	0.81	4.0×10^{15}	5500	5.3×10^{14}	1.39×10^{-14}	0.57
				4.0×10^{14}	2.80×10^{-17}	0.30
$In_{0.53}Ga_{0.30}Al_{0.17}As$	0.98	1.0×10^{15}	4000	4.5×10^{13}	7.18×10^{-18}	0.50
$In_{0.53}Ga_{0.17}Al_{0.30}As$	1.17	1.36×10^{16}	2500	4.8×10^{14}	3.10×10^{-16}	0.64

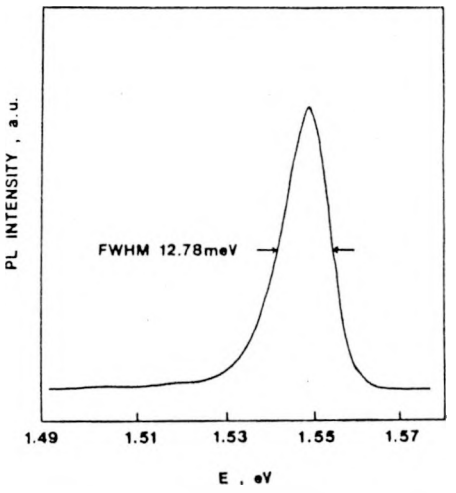

FIG. 1. Low-temperature photoluminescence spectrum of MBE $In_{0.52}Al_{0.48}As$ grown at 1.2 μm/h. $T = 15$ K; $P_{In}/P_{Al} = 3.15$.

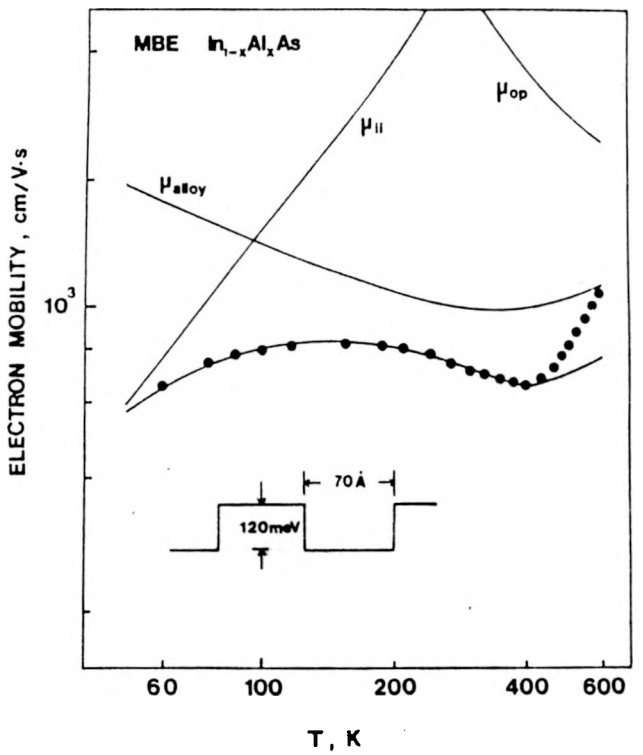

FIG. 3 Measured (dots) and calculated (solid line) temperature-dependent Hall data from $In_{0.52}Al_{0.48}As$. μ_{ii} and μ_{op} are the mobilities limited by ionized impurity scattering and optical phonon scattering, respectively. The estimated composition modulation is shown in the inset.

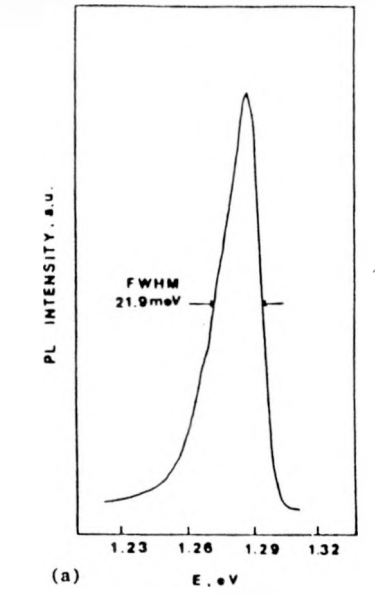

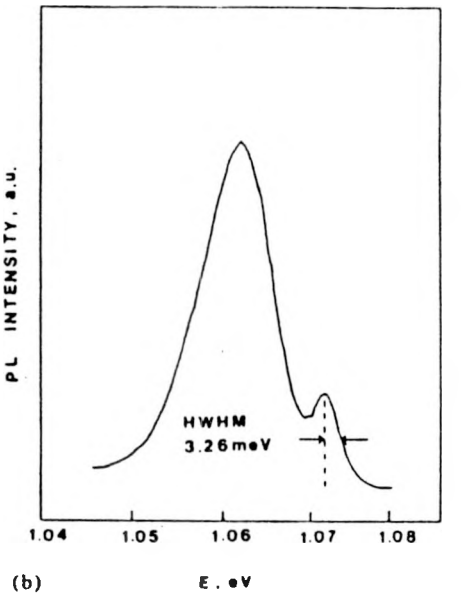

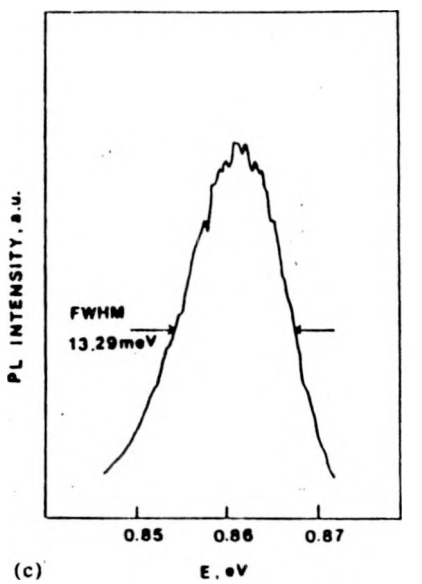

FIG. 2. Low-temperature ($T = 15$ K) photoluminescence spectrum of MBE $In_{1-x-y}Ga_xAl_yAs$ grown at 1.3 μm/h: (a) $In_{0.53}Ga_{0.17}Al_{0.30}As$, (b) $In_{0.53}Ga_{0.30}Al_{0.17}As$, and (c) $In_{0.53}Ga_{0.42}Al_{0.05}As$.

2.2 Minority Carrier Lifetimes

Minority carrier lifetime measurements were made on lightly doped n-type quaternary samples with n=10^{14}-10^{15}cm^{-3}. Photoconductors were made with 10 μm spacing between the contacts. Focused and pulsed (100 ps duration) 830 nm light was used to illuminate the samples and the lifetime was estimated from the photocurrent decay transients. Hole lifetimes of 5 and 12 ns for n-type $In_{0.53}Ga_{0.42}Al_{0.05}As$ and $In_{0.53}Ga_{0.30}Al_{0.17}As$ were measured, respectively. To our knowledge, these are the first measurements of hole lifetimes in these MBE grown quaternaries. The values are comparable to those measured in pure GaAs, and indicate that the materials are relatively pure.

2.3 Non-Random Alloying: Low- and High-Field Transport and Raman Scattering

Experiments based on photoluminescence and carrier transport indicate that the alloy system is not of a high quality and may have alloy clustering present. Although a periodic short-range order as that present in superlattices can be advantageous, clustering generally has a detrimental effect on the optical and transport properties of materials. Due to the large difference between In- and Al-related bond energies the $In_{0.52}Al_{0.48}As$ system is expected to show clustering due to the low temperatures employed in MBE growth. To explain this behavior, we have developed a theoretical formalism for the scattering rate due to alloy clustering. In particular, this scattering can be dominant when the cluster size is much larger than the radius of the Wigner-Seitz cell ($\sim$ 2.5 Å).

The specific experiments performed were high-temperature Hall, low-temperature photoluminescence, x-ray diffraction, high-field transport, determination of the impact ionization coefficients, and Raman scattering.

Room-temperature mobilities in n-type $In_{0.52}Al_{0.48}As$ varied with Si doping, were equal to 3600 cm^2/Vs for a Si doping of 5 $\times$ 10^{15}cm^{-3}, and were 700 cm^2 Vs for a doping of 4.5 $\times 10^{17}$cm^{-3}. The layer thickness was 2-3 μm. In some samples, particularly those with lower mobilities for the same background doping, the mobilities increased with increase of temperature in the range 400-600 K. This is indirect evidence of compositional clustering. We have analyzed the experimental data with a model taking into account mobility limited by nonrandom alloy scattering. A 5% modulation in alloy composition and a cluster size of 70 Å average diameter are estimated. The experimental and calculated data are shown in Fig. 3. Velocity-field curves have also been measured and simulated by Monte Carlo techniques to study the effects of clustering on peak velocity and threshold voltage. The agreement between experimental and calculated data is excellent on using the same cluster

size. The calculated peak velocities decrease with increase of clustering from 1.4 $\times$ 10^7 cm/s without clustering to 5 $\times$ 10^6 cm/s with an enhancement of clustering, as shown in Fig. 4. Fairly good agreement with measured data can be obtained by considering 35 Å alloy clusters of $In_{1-x}Al_xAs$ with x = 0.46 to 0.50. This corresponds to a band-edge potential difference of 120 meV.

Measurement of the impact ionization coefficients in $In_{0.52}Al_{0.48}As$ by ensuring pure electron and hole injection gives $\alpha/\beta \simeq 4$. This result can be explained by considering a modulation of the threshold ionization energies caused by a periodic potential variation of 120 meV.

It should be cautioned that the clustering issue is by no means resolved, and further work is necessary. We have, for example, investigated Raman scattering by LO phonons in InGaAlAs lattice-matched to InP. The dependence of the spectra on x measures, in some sense, the uniformity of the alloys. The Raman data show no evidence of features attributable to regions of different composition in the layers. This and the results in Fig. 5 indicate that, in the length scale probed by RS ($1/q \approx$ 1300 Å; q is the scattering wave vector), clustering is not important in our samples.

2.4 Deep Levels in InAlAs and InGaAlAs on InP

DLTS and optical DLTS measurements were made with a 1 MHz capacitance meter. The measurements were made by scanning the temperature of the sample from 77 to 400 K. Electron and hole traps were identified and characterized by measurements on Schottky diodes and p-n junctions. The work reported here was performed in order to establish whether or not complex defects like the D-X center can be present in InAlAs and to establish the behavior of dominant traps in the quaternary InGaAlAs as a function of the changing bandstructure.

Dominant deep electron and hole traps in lattice-matched $In_{0.52}Al_{0.48}As$/InP have been identified and characterized. The traps have activation energies ranging from 0.25 to 0.95 eV. The electron traps have very large capture cross-sections, $\sim 10^{-12}$-10^{-11} cm^2, similar to attractive centers. The lattice-matched samples do not show any persistent photoconductivity effects at low temperatures. In strained $In_{1-x}Al_xAs$ with $0.48 < x \leq 0.57$, an electron trap with thermal ionization energy of 0.35 eV, a strong dependence of its concentration on donor doping and very small thermal capture cross-section, $10^{-18}cm^{-2}m$ is identified. These samples exhibit persistent photoconductivity. We believe this trap is similar to the D-X center commonly observed in $Al_xGa_{1-x}As$ for $x \geq 0.28$.

Deep level transient spectroscopy measurements have been made on molecular beam epitaxial $In_{0.53}(Ga_xAl_{1-x})_{0.47}As$ lattice-matched to InP. Several electron and

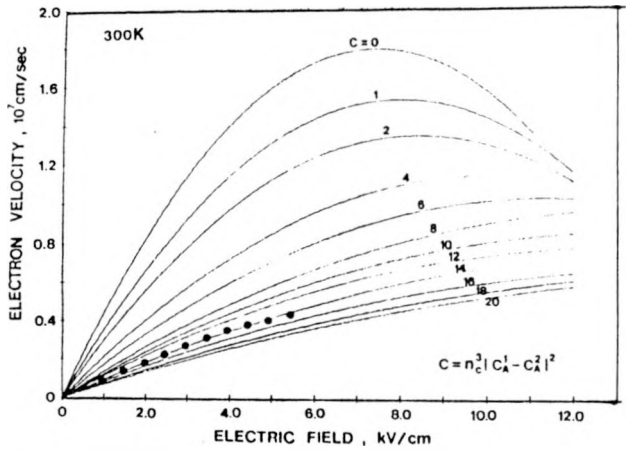

FIG. 4 Calculated and measured velocity-field characteristics in $In_{0.52}Al_{0.48}As$ with random (no clustering: $C = 0$) and nonrandom alloying ($C \neq 0$).

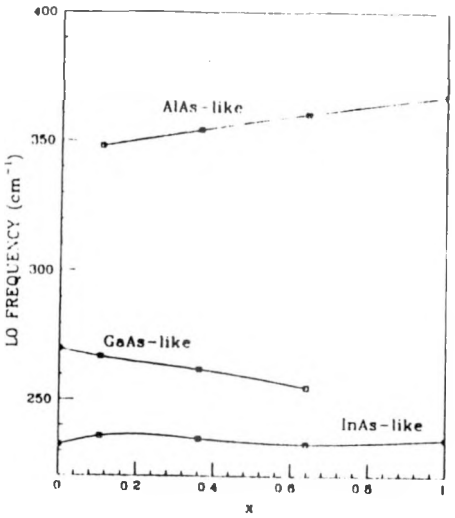

FIG.5 Frequencies of the LO modes as a function of x (the lines are guides to the eye). The data correspond to the spectra shown in Fig. 1. Estimated errors are ± 0.01 for x and ± 2 cm^{-1} for the LO frequencies.

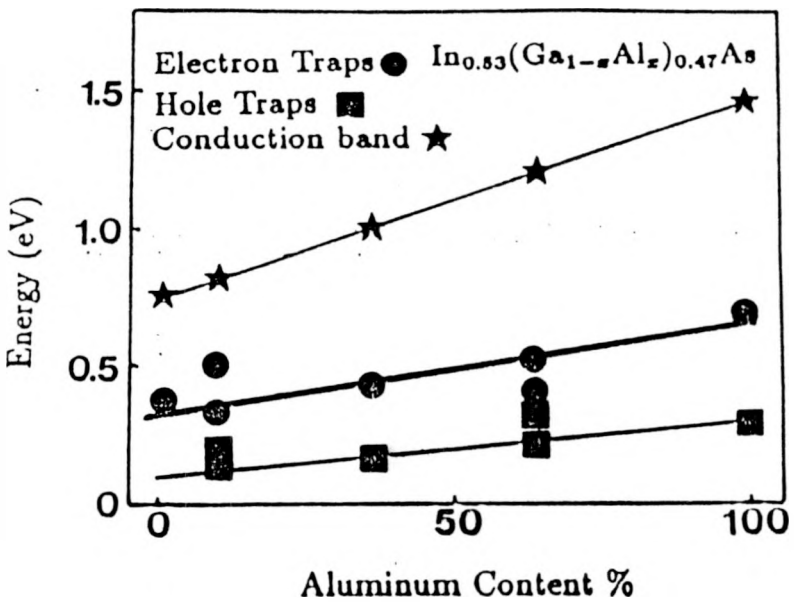

Fig. 6 Measured variation in activation energy of the electron and hole traps with respect to the conduction band edge for different alloy composition of InGaAlAs. The solid lines are joins of the data points.

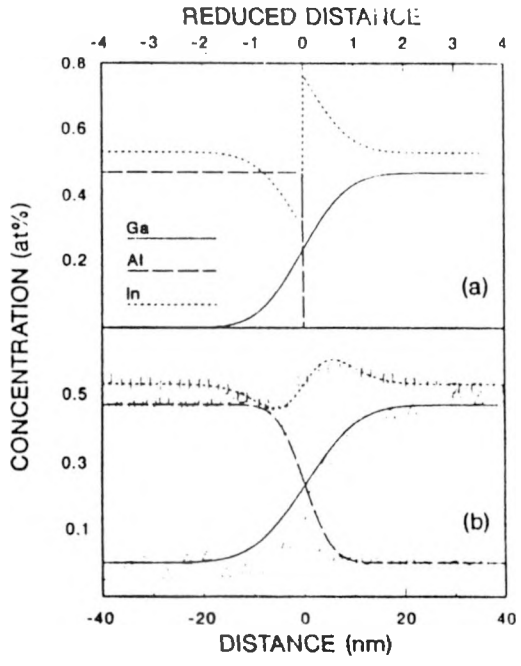

FIG. 7 (a) Calculated group III metal distributions at an annealed $In_{0.53}Ga_{0.47}As/In_{0.52}Al_{0.48}As$ interface for $D_n = 7 \cdot 10^{-15}$ cm^2/s and $t = 36000$ s. The scale at the top of the figure is in reduced distance ($x/\sqrt{4D_n t}$). (b) Profiles from (a), broadened by convolution with a Gaussian of 10 nm FWHM to simulate the experimental depth resolution, plotted over the experimental data points [(□) = In, (○) = Al, and (△) = Ga]. Only every other data point is shown for clarity.

hole traps, with activation energies ranging from 0.14 eV to 0.79 eV have been identified and characterized. In particular, systems of electron traps ($0.30 \leq \Delta E_T \leq 0.79$ eV) and hole traps ($0.14 \leq \Delta E_T \leq 0.31$ eV) with monotonically changing activation energies have been identified in these alloys (Fig. 6). We believe these traps are dominant in this alloy system.

III. INTERDIFFUSION AND IMPURITY-INDUCED DISORDERING PHENOMENA IN InGaAs/InAlAs HETEROSTRUCTURES AND SUPERLATTICES

We have measured, by Auger compositional depth profiling, the interdiffusion of group III metals at annealed $In_{0.53}Ga_{0.47}As/In_{0.52}Al_{0.48}As$ interfaces. We find, rather than the simple Al/Ga interdiffusion that had been assumed in a prior study, a more complex behavior in which In and Ga interdiffuse against an essentially constant Al concentration profile. This behavior, which leads to a near discontinuity in the In concentration at the location of the original interface, can be rationalized if one assumes that the mobilities of the group III metals are inversely related to their bonding strength in the lattice, i.e., the mobilities are ordered In > Ga > Al. In this case, Ga diffusion is driven by the Ga concentration gradient; and In, which is more mobile than the Al, diffuses in the chemical potential gradient established by the disparity between the Ga and Al mobilities and the requirement of stoichiometry. This effect is general to interdiffusion at multicomponent interfaces where the mobilities of the diffusing species differ. A similar effect was first observed in solids by Darken for the interdiffusion of carbon and silicon in iron[7].

The interdiffusion experiments were carried out on $In_{0.53}Ga_{0.47}As/In_{0.52}Al_{0.48}As$ heterostructures grown by molecular beam epitaxy (MBE) on semi-insulating, Fe-doped InP substrates. They consisted of a single 100 nm layer of $In_{0.53}Ga_{0.47}As$ in an $In_{0.52}Al_{0.48}As$ matrix. The samples were uniformly lightly doped with Si to provide electrical conductivity which prevented sample charging during Auger depth profiling. Isothermal annealing of the samples was carried out in a horizontal furnace under flowing nitrogen at 1085 K. The measured concentration profiles were analyzed with a simple error-function diffusion model. The experimental and calculated profiles are shown in Fig. 7. These results imply that there may be serious problems resulting from such interdiffusion, in that the interface regions will develop biaxial strain due to the excess In accumulation.

Impurity-induced layer disordering of $In_{0.53}Ga_{0.47}As/In_{0.52}Al_{0.48}As$ heterostructures grown by molecular beam epitaxy has been observed by Auger electron spectroscopy depth profiling. We find that Si^+ ion implantation to concentrations greater than 2×10^{19} atoms cm^{-3} enhances the intermixing of Ga and Al in these heterostructures at an annealing temperature of 1075 K. However, the relatively

high temperature which is required to activate the interdiffusion of Ga and Al in the region of high Si concentration is sufficient to induce In diffusion in regions of lower Si concentration. Zinc diffusion is found to completely intermix the Ga and Al in the heterolayers at temperatures as low as 825 K, which is below the temperature at which significant In diffusion occurs in undoped regions.

IV. MBE OF STRAINED $In_xGa_{1-x}As$ ON GaAs: GROWTH PHENOMENA AND DISLOCATIONS

4.1 Initial Stages of MBE Growth and Growth Modes

A detailed study of reflection high energy electron diffraction (RHEED) during growth of $In_xGa_{1-x}As$ ($0 \leq x \leq 0.5$) on GaAs was carried out. We focussed on the initial stages of growth where the growth is expected to be under coherent strain. RHEED studies provide us information on the growth front which is quite different from what is found in the lattice matched systems. In lattice matched systems, as the growth temperature is increased, the growth front becomes increasingly smooth (below congruent temperature) due to the enhanced surface kinetics. however, in the presence of strain we find that increased substrate temperature produces a growth front which is 3-dimensional in nature. This effect is explained by the reasoning that the equilibrium surface for the lattice matched systems are automatically smooth and that for a strained surface can be 3-dimensional depending upon surface strain.

In Fig. 8 we show the initial states of RHEED oscillations as growth of InGaAs is initiated on an on-axis smooth GaAs. Note the extremely rapid decay of the oscillations clearly suggesting that while in the lattice matched region of the growth (GaAs on GaAs) the RHEED oscillations show a layer by layer growth. In the strained case the growth mode abruptly changes to a 3-d island mode. We also see that as the strain (In composition) is increased, the transition to the 3-d mode is most abrupt. Note that in all cases shown the epilayer thickness is below the critical thickness, consistent with the theoretical arguments presented above, and suggest that the close-to-equilibrium surface for the strained epilayer is indeed 3-d in nature.

Figure 9 depicts RHEED oscillation data during growth of $In_{0.2}Ga_{0.8}As$ on GaAs at various substrate temperatures. Very few periods of oscillation are observed at 400°C. This is because the nucleation rate of the epilayer is much faster than the surface diffusion rate at a lower temperature. The average intensity of the RHEED pattern is stronger, but rather more diffuse at the lower epitaxial growth temperatures. This result suggests that the intial stage of the epilayers grown at lower temperatures have relatively smoother surfaces, but a lower surface crystallinity than those grown at elevated temperatures.

In Fig. 10 we show the change in surface lattice constants as obtained from the RHEED integral order spacings. By analysis of the dynamic changes of these peaks, we see dramatic movement at higher temperatures near the Ball, Van der Merwe critical thickness of 34.5 Å. It should be noted that the theory of Ball, Van der Merwe predicts that under thermodynamic equilibrium an epilayer should maintain the substrate's lattice constant until it becomes energetically favorable to produce misfit dislocations to relieve the strain energy. When dislocations are produced, a spontaneous change in the epilayer lattice constant is expected. At low temperatures where impinging atoms are unable to move in a correlated manner to reach the free energy minimum surface, the lattice constant remains close to the substrates. However, at higher temperatures as the surface kinetics is increased, the monotonic change of the lattice constant expected from the simple energy balance treatment is indeed observed.

We have now conclusively established that for misfits $\geq 1.5\%$, a 3-d island mode of growth is energetically favored. This has also been theoretically calculated from strain energy considerations. The implications of this result is serious. A 3-D growth front would seriously degrade heterointerfaces in active devices. Since the surface reconstruction under Group V stabilized growth is largely responsible, one needs to go to other growth modes such as migration enhanced epitaxy (MEE) where the growth front is alternately Group V and Group III stabilized.

4.2 Dislocation Formation and Optical Properties of Multiquantum Wells

We have investigated the generation and propagation of misfit dislocations in strained $In_yGa_{1-y}As/GaAs$ multiquantum wells grown by molecular beam epitaxy, with cross-sectional transmission electron microscopy. The samples are of excellent optical quality, with multiquantum wells having well widths of 100 Å, being characterized by excitonic linewidths and Stokes shifts of 1.5-2.5 and 1-2 meV, respectively. We have examined the growth of 2 μm-thick multiquantum well samples grown either directly on GaAs, or with an intermediate composition buffer layer, and for the cases of small (y=0.07) and large (y=0.16) misfits. It is seen that for the case of quantum wells with small misfit, grown directly on GaAs, metastable growth can be achieved. This is confirmed by low-temperature absorption measurements and from transmission electron microscopy experiments performed both before and after post-growth thermal annealing. In the case of quantum wells with large misfits directly grown on GaAs, dislocations are generated within the first few periods, and high optical quality is retained in the subsequent free-standing quantum wells. In the case of quantum wells grown with an intermediate composition $In_xGa_{1-x}As$ buffer layer, dislocations are generated at the buffer-GaAs interface, and the freestanding multiquantum well is again of very high quality.

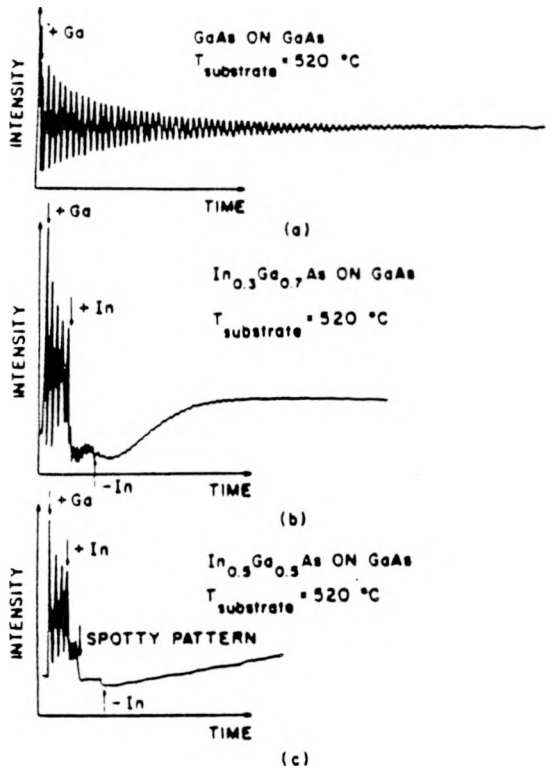

Figure 8 RHEED oscillation for growth of (a) GaAs on GaAs, (b) $In_{0.3}Ga_{0.7}As$ on GaAs and (c) $In_{0.5}Ga_{0.5}As$ on GaAs.

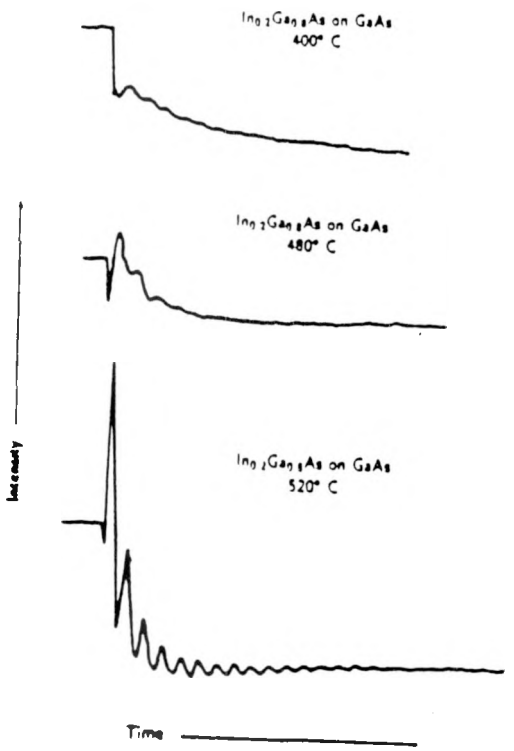

Figure 9 RHEED oscillation data for growth of $In_{0.2}Ga_{0.8}As$ on GaAs at various temperatures.

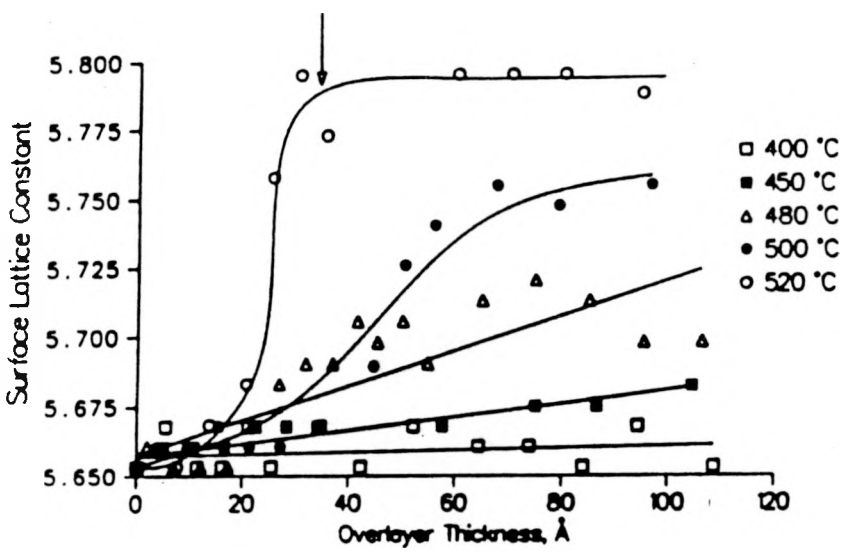

Figure 10 Surface lattice constant measured by RHEED integral order spacing with increasing overlayer thickness of MBE grown $In_{0.35}Ga_{0.65}As$ on GaAs at various substrate temperatures.

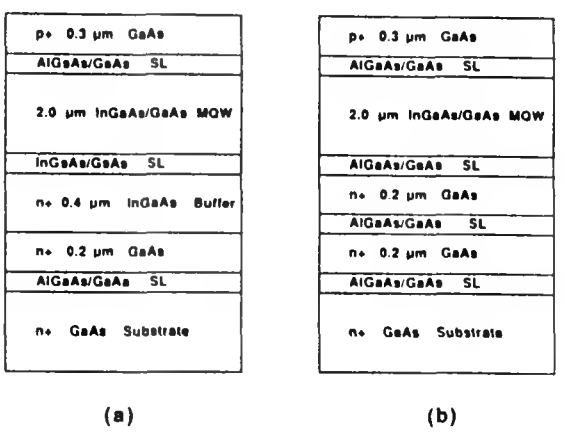

FIG.11 Schematic diagrams of strained MQW structures grown by M (a) with and (b) without intermediate composition buffer.

Schematics of the strained heterostructures grown by MBE are shown in Fig. 11. The fabrication of XTEM specimens was made by gluing together six 5 × 5 mm^2 GaAs wafers face-to-face with epoxy resin (only the center two were processed). The wafer blocks were sliced by a diamond saw on <110> cleavage directions. The cross-sectional slices were polished, dimpled, and then ion milled to transparency. The specimens were examined in a JEOL 2000FX transmission electron microscope operating at 200 kV. Cross-sectional TEM micrographs are shown in Figs. 12 and 13.

4.3 Characteristics of Dislocations at Strained InGaAs/GaAs Heterointerfaces

We have shown by detailed TEM analysis the formation, interaction and propagation of misfit dislocations at an MBE-grown InGaAs/GaAs heteroepitaxial interface. With the strain systems less than 2% lattice mismatch, the majority of the misfit dislocations are confined at the same heterointerface after the elastic strain relaxation. Most of the misfit dislocations are found to be mixed dislocations with Burgers vector of a/2 <110> type at 60° to the dislocation line. Sessile type edge dislocations can also originate from the combination of two 60° mixed dislocations. Numerous sessile edge dislocations were generated during the later part of the elastic strain relaxation through climb or interaction processes. The interfacial dislocation network is found to contain regions of dislocation with the same Burgers vector that extend over several micrometers. The interfacial dislocation multiplication process proposed by Hagen and Strunk[8] is the most probable mechanism for this grouping character of the misfit dislocations.

For large lattice-mismatched systems ($\epsilon \leq 2\%$), the majority of the misfit dislocations are pure edge dislocations. This process occurs because island growth is favored over two-dimensional layer-by-layer growth, and the edge dislocations are often formed by island coalescence at the initial epitaxial growth. A high threading dislocation density in the InGaAs layer is generally found in the large mismatched systems. We believe this may be due to the threading of the tails fo the dislocation half loop and the transition dislocation segments of a Hagen-Strunk multiplication process. In conclusion, it is apparent that very low threading dislocation density $In_xGa_{1-x}As$ films with $x < 0.2$ can be grown on GaAs by MBE when the dislocation multiplication mechanism operates. From the understanding of the interfacial dislocation multiplication process, new growth parameters can be developed, which will be useful for realizing heterostructures devices with large mismatch.

The general nature of the misfit dislocation network at the $In_{0.15}Ga_{0.85}As$/GaAs interface is an asymmetrical orthogonal array as shown in Fig. 14. This asymmetry is due to the absence of inversion symmetry in the zincblende lattice. Figure

15 shows several different dislocation interactions at the InGaAs/GaAs interface. A schematic diagram of these reactions is shown in Fig. 16. It is found that at the intersection point *O* in Fig. 16 two 60° mixed dislocations, each having the same Burgers vector, interact with each other to eliminate the crossing point and reduce the line energy of the dislocation. A suitable explanation of this dislocation multiplication process has been given by Hagen and Strunk. These authors have reported that there can be a sizable repulsive interaction of two orthogonal 60° mixed dislocations with identical Burgers vector. This repulsive reaction can lead to the formation of two angular dislocations in an aymmetric configuration. Dislocation propagation phenomena is highlighted in the XTEM micrograph of Fig. 17.

A significant result obtained in this study is the correlation between the surface cross-hatched morphology (Fig. 18) and the interfacial misfit dislocations. The surface pattern is clearly seen on samples grown at high temperature (520°C) and those with small lattice-mismatched (f < 2%) systems. A poorly defined cross-hatched morphology was found on layers grown at relatively low temperature (400°C). As the lattice mismatch of the strained layer becomes larger than 2%, a roughly textured surface morphology is commonly observed in place of actual cross hatching. Few threading dislocations are observed in the strained layer when the cross-hatched pattern develops. It is also noted that the surface cross-hatched pattern develops after the majority of the interfacial misfit dislocations are generated. The result suggests that the surface cross-hatched pattern is directly related to the generation of interfacial misfit dislocations through glide processes. Details of this work can be found in the listed manuscript submitted for publication in Journal of Applied Physics.

4.4 Structural Properties of Other Mismatched Heterostructures

Theoretical and experimental aspects of the growth of GaAs/Al/GaAs heterostructures have been investigated. In these heterostructures the GaAs on top of the buried metal layer is grown by migration enhanced epitaxy at low temperature (200 and 400°C) to provide a kinetic barrier to the outdiffusion of Al during superlayer growth. The crystallinity and orientation of the Al film itself deposited on (100) GaAs at ~ 0° was studied by transmission electron diffraction, dark field imaging, and X-ray diffraction measurements. It is found that the Al growth is polycrystalline with a grain size ~ 60 Å and the preferred growth orientation is (111), which may be textured in plane but oriented out of plane. The quality of the GaAs superlayer grown on top of Al by MEE is very sensitive to the growth temperature. The layer grown at 400°C has good structural and optical quality, but is accompanied by considerable outdiffusion of Al at the Al-GaAs heterointerface. At 200°C where the interface has good structural integrity, the superlayer exhibits twinning and no luminescence is observed.

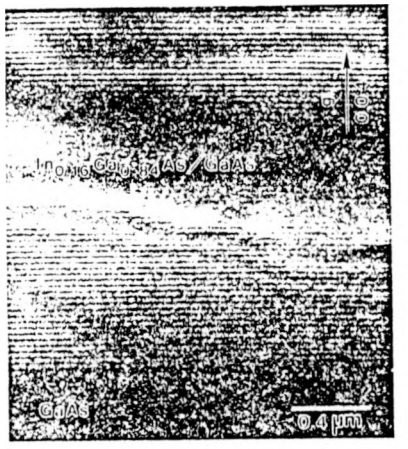

Fig. 12 XTEM micrographs of a 2 μm InGaAs/GaAs MQW.

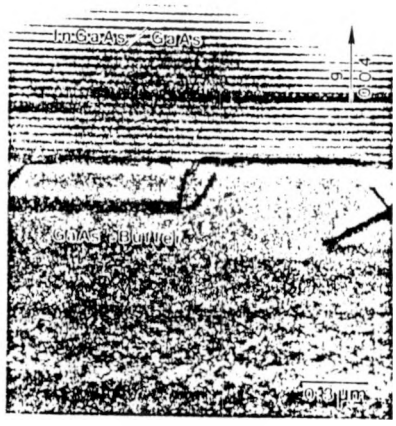

Fig. 13 XTEM micrographs of the details of interfacial defects.

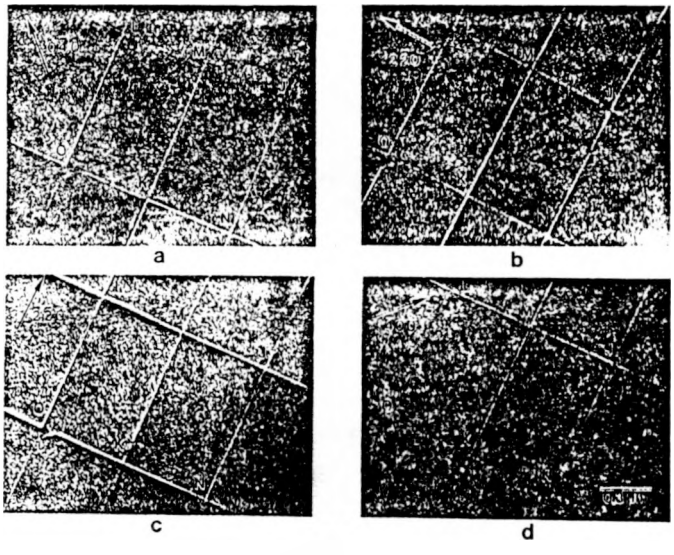

Fig. 14 Weak beam images of the dislocation interactions at the InGaAs/GaAs heteroepitaxial interface. As showing at crossing points J and K, no reaction occurs for two dislocations with perpendicular Burgers vectors. Interaction between two dislocations with 60° inclined Burgers vectors generate new screw character segments L, M, and N. The crossing point O shows two dislocations with identical Burgers vectors interacting with each other. The diffraction conditions are (a)$g_{0\bar{4}0}$, (b)$g_{2\bar{2}0}$, (c)$g_{11\bar{3}0}$, and (d)g_{400}.

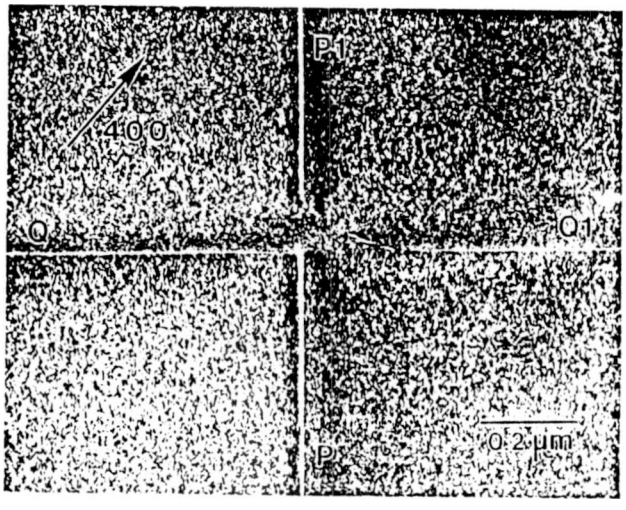

Fig. 15 TEM image of the repulsive reaction between two 60° mixed dislocations with the identical Burgers vectors. Two split dislocations with inclined screw segments are generated after the glide dislocations reach the film surface.

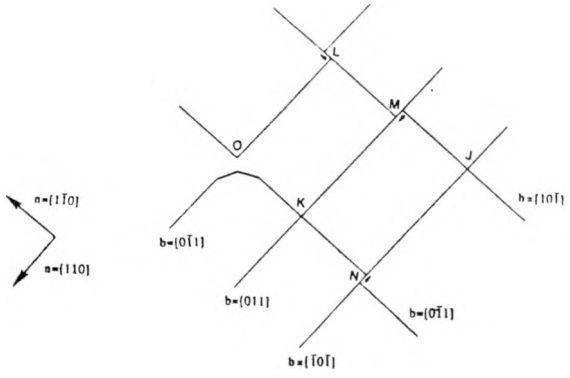

FIG. 16 Schematic illustration of the different dislocation interactions shown in Fig. 5.

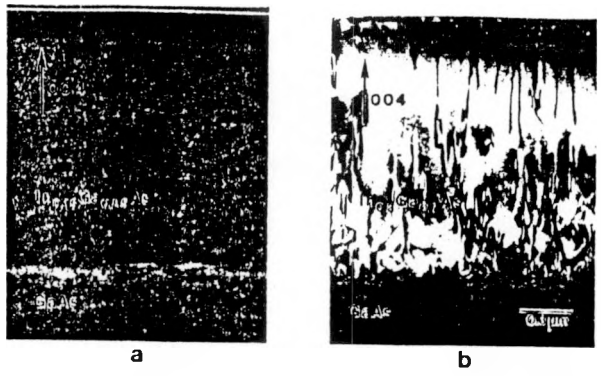

Fig. 17 Cross-sectional TEM micrograph of $In_xGa_{1-x}As/GaAs$ heteroepitaxial structure for (a) $x = 0.15$ and (b) $x = 0.30$.

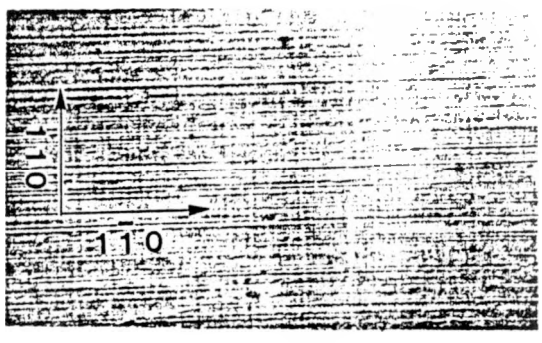

(a) (100) GaAs.

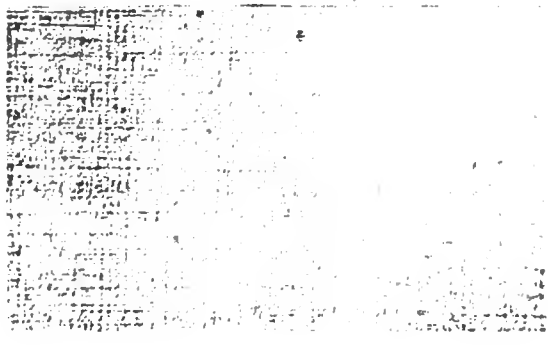

(b) 2° off (100) GaAs.

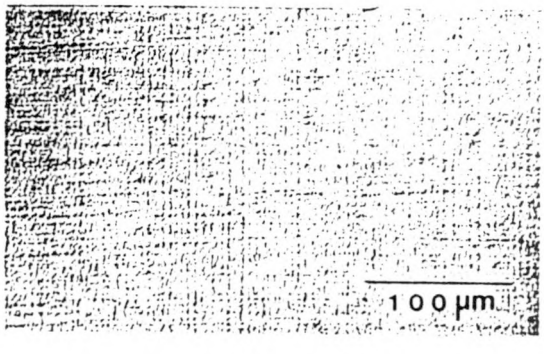

(c) 4° off (100) GaAs.

Fig. 18 **Surface Morphology of $In_{0.15}Ga_{0.85}As/In_{0.15}Al_{0.85}As$ MQW on GaAs.**

We have also evaluated the structural and optical properties of GaAs grown by molecular beam epitaxy on (0001) and $(01\bar{1}2)$-oriented sapphire substrates for possible direct deposition on sapphire optical fibers and optoelectronic device applications. X-ray diffraction studies and cross-sectional transmission electron microscopy measurements show that the GaAs films are single-crystal and have a (111) orientation for both substrate orientations. Both x-ray and temperature-dependent photoluminescence measurements indicate that the quality of the GaAs films is better for the $(01\bar{1}2)$ sapphire orientation. Post growth short term halogen lamp annealing marginally improves the overall luminescence intensity of the samples. A linewidth of 20 meV is measured for a (80 Å) GaAs/(120 Å) $Al_{0.3}Ga_{0.7}As$ multiquantum grown on sapphire. From this initial study it is apparent that device-quality single-crystal GaAs and GaAs-related compounds can be deposited directly on sapphire substrates by molecular beam epitaxy, using special growth techniques.

V. DEVICE APPLICATIONS OF STRAINED LAYERS

We have applied the knowledge gained from the growth and dislocation studies on mismatched layers to two kinds of high-speed electronic devices. The first is a $In_{0.53}Ga_{0.47}As/In_{0.52}Al_{0.48}As$ modulation-doped field effect transistor (MODFET) on a GaAs substrate (with a 3.5% mismatch). The generation and propagation of misfit dislocations are controlled by the incorporation of successive mismatched $In_xGa_{1-x}As$ layers with varying degrees of mismatch ($0 \leq x \leq 0.53$). In the second device, a bipolar transistor, pseudomorphic InGaAs quantum wells are incorporated at the base-collector junction to artificially enhance the electron/hole multiplication ratio. This greatly enhances the gain of the transistor. The modulation-doped heterostructures are characterized by μ_{300K} = 8,150 $cm^2/V.s$ ($n_s = 2.7 \times 10^{12} cm^{-2}$) and μ_{20K} = 26,100 $cm^2/V.s$ ($n_s = 2.1 \times 10^{12}$ cm^{-2}) which compare very favorably with values measured in similar lattice-matched heterostructures on InP. 1.4 μm gate MODFETs exhibit g_m (ext) = 240 mS/mm and f_T = 21 GHz. The drain current variation with gate bias is linear and the transconductance is uniform over a sizeable voltage range. These material and device characteristics indicate that $In_xGa_{1-x}As/In_xAl_{1-x}As$ MODFETs (with x varying over a certain range to vary ΔE_c) can be designed on GaAs or even other mismatched substrates.

In the GaAs/AlGaAs/InGaAs phototransistor three periods of a periodic pseudomorphic structure, in which electrons should predominantly multiply, are included in the collector depletion region. Independent measurements of the electron and hole avalanche multiplication rates, M_n and M_p, in these structures confirm that M_n/M_p and α/β are $\sim$ 2-4, depending on bias voltage. The observed photocurrent characteristics agree reasonably well with Monte Carlo calculations made to simulate the transport of electrons through the collector region. Measured opti-

cal gains are as high as 142 in an n-p-n phototransistor with a 2000 Å p-base region.

VI. CONCLUSIONS

The research described here, extending over a period of three years has enabled us to gain a better understanding of the electrical, optical and structural properties of In-bearing lattice-matched and strained alloy semiconductors. Important understanding has been achieved on the MBE growth of these compounds, which has far-reaching consequences on device design and performance. Our results imply that in using highly strained layers as active regions of electronic and optoelectronic devices, other growth modes and growth techniques need to be investigated. The issue of clustering in these alloys, which we have identified and characterized, needs to be resolved and eliminated.

We have gained a good understanding of the generation of interfacial misfit dislocations in strained heterostructures and their dependence on the growth conditions. More importantly, we now understand how they propagate and multiply along the growth front. With this knowledge we have been able to obtain electronic properties in highly strained (3.5%) active layers which are almost identical to the corresponding lattice-matched ternary semiconductors.

The project has greatly benefited from the interactions with several of our colleagues, and in particular Professor J. Singh of the EECS Department, and Professor D. Srolovitz and Dr. J. Mansfield of the MSE Department. The support of the technical personnel in the EMAL and SSEL is gratefully acknowledged.

VII. PUBLICATIONS AND CONFERENCE PRESENTATIONS

1. "Non-Random Alloying in $In_{0.52}Al_{0.48}As/InP$ Grown by Molecular Beam Epitaxy," W-P. Hong, P. K. Bhattacharya and J. Singh, *Applied Physics Letters*, **50**, 618 (1987).

2. "Deep Levels and a Possible D-X Like Center in Molecular Beam Epitaxial $In_xAl_{1-x}As$," W-P. Hong, S. Dhar, P. K. Bhattacharya and A. Chin, *Journal of Electronic Materials*, **16**, 271 (1987).

3. "Material Properties and Clustering in Molecular Beam Epitaxial $In_{0.52}Al_{0.48}As$ and $I_{1-x-y}Ga_xAl_yAs$," W-P. Hong, A. Chin, N. Debbar, J. Hinckley, P. K. Bhattacharya, J. Singh and R. Clarke, *J. Vac. Sci. Technol.* B**5**(3), 800 (1987).

4. "Growth and Properties of $In_{0.52}Al_{0.48}As/In_{0.53}Al_{0.47}As$, GaAs: In and InGaAs/GaAs Multilayers," Presented at the 7th International MBE Workshop, York, September 1986.

5. "Molecular Beam Epitaxial Growth and Luminescence of $In_xGa_{1-x}As/In_xAl_{1-x}As$ Multiquantum Wells on GaAs," K. Chang, P. R. Berger, J. Singh and P. K. Bhattacharya, *Appl. Phys. Lett.* **51**, 261 (1987).

6. "Molecular Beam Hetero-Epitaxial Growth of InGaAs/InAlAs Multiquantum Wells on GaAs with In-Situ RHEED Studies," K. H. Chang, P. R. Berger, P. K. Bhattacharya, J. Singh, D. C. van Aken and R. Gibala, presented at the Electronic Materials Conference, Santa Barbara, June 1987.

7. "Molecular Beam Epitaxial Growth of High-Quality $In_{0.52}Al_{0.48}As$ and $In_{1-x-y}Ga_xAl_yAs$," Albert Chin and Pallab Bhattacharya, *Journal of Vac. Sci. and Technol.*, **B6**(2), 665 (1988).

8. "Dislocation Studies of Molecular Beam Hetero-Epitaxial Growth of Strained InGaAs on GaAs," K. H. Chang, J. F. Mansfield, R. Gibala, P. R. Berger, P. K. Bhattacharya and J. Singh, 1988 TMS/AIME Annual Meeting.

9. "Raman Spectroscopy of $In_{1-x-y}Ga_xAl_yAs$ Alloys," A. Chin, P. Bhattacharya, R. Boroff and R. Merlin, *Appl. Phys. Letters*, **53**, 1652 (1988).

10. "The Relationship of the D-X center in $Al_xGa_{1-x}As$ and other III-V alloys with the conduction band structure," Semiconductor Science and Technology, **3**, 1145 (1988).

11. "Indium Diffusion in the Chemical Potential Gradient at an $In_{0.53}Ga_{0.47}As/In_{0.52}Al_{0.48}As$ Interface," R. J. Baird, T. J. Potter, R. Lai, G. Kothiyal and P. K. Bhattachaya, *Appl. Phys. Letters*, **52**, 2055 (1988).

12. "Impurity-Induced Layer Disordering in $In_{0.53}Ga_{0.47}As/In_{0.52}Al_{0.48}As$ Heterostructures," R. J. Baird, T. J. Potter, R. Lai, G. Kothiyal and P. K. Bhattacharya, *Appl. Phys. Lett.* **53**, 2302 (1988).

13. "Molecular Beam Hetero-Epitaxial Growth of Strained InGaAs on GaAs," K. H. Chang, P. R. Berger, R. Gibala, P. K. Bhattachayra, J. Singh, J. F. Mansfield and R. Clarke, Proceedings of the Symposium on Dislocations and Interfaces in Semiconductors, Phoenix, Arizona, January 1988, (eds. Rajan, Narayan and Ast), The Metallurgical Society, 1988, pp. 157-171.

14. "In-Situ RHEED Studies to Understand the Dislocation Formation Process in Growth of InGaAs on GaAs," P. R. Berger, K. H. Chang, P. Bhattacharya, J. Singh and K. K. Bajaj, Presented at the SPIE Conference on Growth of Compound Semiconductor Heterostructures, Newport Beach, CA, March 1988.

15. "Growth Phenomena and Characteristics of Strained $In_xGa_{1-x}As$ on GaAs," J. Pamulapati, P. Berger, K. Chang, J. Oh, Y. Chen, J. Singh, P. K. Bhattacharya and R. Gibala, *Jour. of Crystal Growth*, **95**, 193 (1989).

16. "Transmission Electron Microscopy of Strained $In_yGa_{1-y}As/GaAs$ Multiquantum Wells: The Generatioon of Misfit Dislocations," K. H. Chang, P. K. Bhattacharya and R. Gibala, *J. Appl. Physics*, **65**, 3391 (1989).

17. "Characteristics of Dislocations at Strained Heteroepitaxial InGaAs/GaAs Interfaces," K. H. Chang, P. K. Bhattacharya and R. Gibala, *J. Appl. Physics*, **66**, 2993 (1989).

18. "Optical and Structural Properties of Molecular Beam Epitaxial GaAs on Sapphire," A. Chin, P. K. Bhattacharya, K. H. Chang and D. Biswas, *J. Vac. Sci. Technol.*, B7(2), 283 (1989).

19. "Theory and Operation of a GaAs/AlGaAs/InGaAs Superlattice Phototransistor with Controlled Avalanche Gain," A. Chin and P. Bhattacharya, *IEEE Transactions on Electron Devices*, **36**, 2183 (1989).

20. "Traps in Molecular Beam Epitaxial $In_{0.53}(Ga_xAl_{1-x})_{0.47}As/InP$," D. Biswas, A. Chin, J. Pamulapati and P. Bhattacharya, *Journal of Applied Physics*, submitted for publication.

21. "Growth and Characterization of GaAs/Al/GaAs Heterostructures," P. Bhattacharya, J. E. Oh, J. Singh, D. Biswas, R. Clarke, W. Dos Passos, R. Merlin, N. Mestres, K. H. Chang and R. Gibala, *Journal of Applied Physics*, submitted for publication.

22. "Lattice-Mismatched $In_{0.53}G_{0.47}As/In_{0.52}Al_{0.48}As$ MODFETs on GaAs: MBE Growth and Device Performance," K. Chang, P. Bhattacharya and R. Lai, *Journal of Applied Physics*," submitted for publication.

23. "Cross-Hatched Surface Morphology in Strained III-V Semiconductor Films," K. H. Chang, R. Gibala, D. J. Srolovitz, P. Bhattacharya and J. F. Mansfield, *Journal of Applied Physics*, submitted for publication.

24. "Surface Cross-Hatched Morphology on Strained III-V Semiconductor Heterostructures," K. H. Chang, R. Gibala, D. J. Srolovitz, P. K. Bhattacharya and J. F. Mansfield, Proceedings of the Annual MRS Meeting, Boston, November 1989.

VIII. Ph.D THESES

1. K. H. Chang, "Molecular Beam Epitaxial Growth and Characterization of Strained InGaAs/GaAs Heterostructures," Department of Materials Science and Engineering, University of Michigan, 1989, Co-chairs: R. Gibala and P. K. Bhattacharya.

2. F-D. Albert Chin, " Studies on Molecular Beam Heteroepitaxy and Controlled Avalanche Superlattice Transistors," Department of Electrical Engineering and Computer Science, University of Michigan, 1989. Chair: P. K. Bhattacharya.

IX. REFERENCES

1. K. Y. Cheng, A. Y. Cho, T. J. Drummond and H. Morkoc, *Appl. Phys. Lett.* **40**, 147 (1982).

2. D. F. Welch, G. W. Wicks and L. F. Eastman, *Appl. Phys. Lett.* **43**, 762 (1983).

3. J. H. Marsh, *Appl. Phys. Lett.* **4**, 732 (1982).

4. N. Holonyak, W. D. Laidig, M. D. Camras, H. Morkoc, T. J. Drummond, K. Hess and M. S. Burroughs, *J. Appl. Phys.* **52**, 7201 (1981).

5. N. Holonyak, W. D. Laidig, B. A. Vojak, K. Hess, J. J. Coleman, P. D. Dapkus and J. Bardeen, *Phys. Rev. Lett.* **45**, 1703 (1980).

6. K. S. Seo, P. K. Bhattacharya, G. P. Kothiyal and S. Hong, *Appl. Phys. Lett.* **49**, 966 (1986).

7. L. S. Darken *Trans. AIME*, **180**, 430 (1949).

8. W. Hagen and H. Strunk, *Appl. Phys. Lett.* **17**, 85 (1978).